



An uncertainty propagation method for multimodal distributions through unimodal decomposition strategy

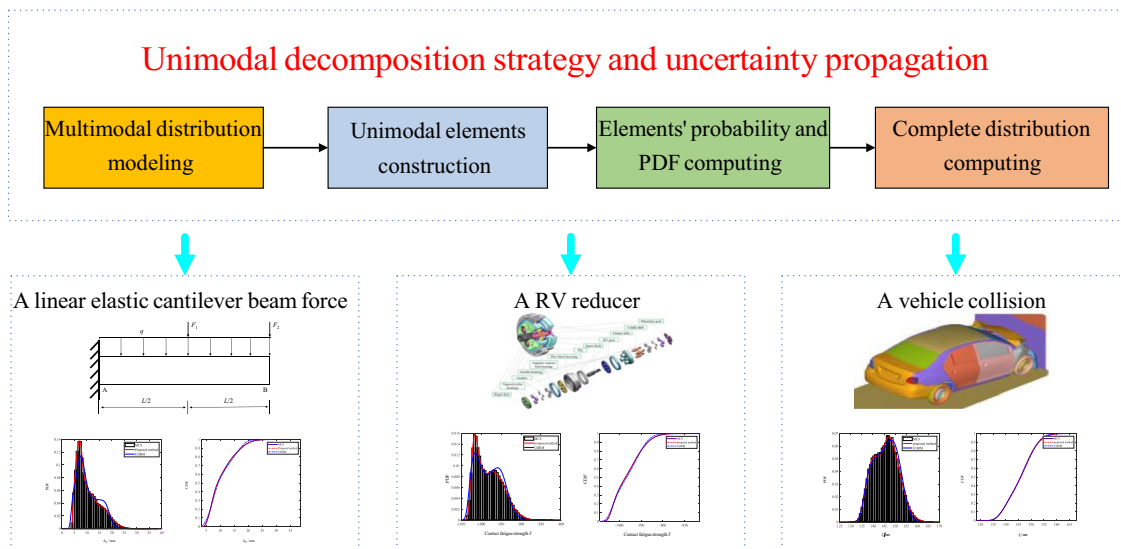
Boqun Xie¹ · Chao Jiang¹ · Zhe Zhang¹ · Jing Zheng¹ · Jinwu Li¹

Received: 21 November 2022 / Revised: 11 May 2023 / Accepted: 13 May 2023 / Published online: 6 June 2023
© The Author(s), under exclusive licence to Springer-Verlag GmbH Germany, part of Springer Nature 2023

Abstract

In practical engineering problems, random variables may follow a multimodal distribution. Traditional uncertainty propagation methods may yield poor effectiveness for multimodal distribution problems. In this paper, an uncertainty propagation method is proposed for multimodal distributions via a unimodal decomposition strategy. First, a Gaussian mixture model is used to build the probability density function of multimodal random variables. Second, a set of unimodal elements is constructed based on the decomposed multimodal random variables. In this way, it avoids computing higher-order statistical moments and the first 4th-order statistical moments can satisfy the accuracy requirements. Third, the probability density function of the response function in each element is computed using an arbitrary polynomial chaos expansion and the maximum entropy method. Finally, the probability density function of the response function in the complete probability space can be obtained by accumulating the probability density functions of the response functions in the elements. Three examples are investigated to validate the effectiveness of the proposed method.

Graphical abstract



Keywords Multimodal random variables · Uncertainty propagation · Unimodal decomposition strategy · Arbitrary polynomial chaos expansion

Responsible Editor: Yoojeong Noh

Extended author information available on the last page of the article

1 Introduction

Uncertainties widely exist in engineering problems, such as inhomogeneous materials (Bai and Kang 2021), manufacturing errors (Zhao et al. 2019; Qiao et al. 2021), random loads (Liu et al. 2021a; Wu and Law 2012), and so on. Uncertain parameters can lead to large fluctuations in the structural response and lead to reliability problems. Therefore, it is necessary to determine the distributional properties of the response function and provide the probability density function of the response function for reliability optimization design (Liu et al. 2021b; Wang and Luo 2019; Tian et al. 2022; Tang et al. 2022). Uncertainty propagation methods are commonly developed based on probability statistics theory, which can obtain the uncertainty information of the response function, such as the probability density function (PDF), cumulative distribution function (CDF), mean, and variance. At present, numerous significant achievements have been made for uncertainty propagation problems, which can be roughly divided into two categories: sampling-based methods and moment-based methods. The sampling-based methods, such as the Monte Carlo simulation (MCS) method (Grigoriu 1984; Marseguerra et al. 1998), are extensively used in uncertainty propagation. A large number of samples are used to compute the response function. They can achieve satisfactory computational accuracy, but are relatively less computationally efficient. Therefore, they are not suitable for practical problems. Some modified methods, such as importance sampling methods (Mori and Kato 2003) and subset simulation (Au and Beck 2001; Bourinet et al. 2011), have been proposed to improve the computational efficiency of the sampling-based methods. However, the low computational efficiency has been a problem for these methods. Therefore, the moment-based methods have been proposed with satisfactory computational efficiency.

Moment-based methods include numerical integration methods, function expansion methods, and local expansion methods. Numerical integration methods are used to compute the statistical moments of the response function based on a limited number of integration points and weights, which include the dimension reduction methods (Rahman and Xu 2004; Xu and Rahman 2004) and sparse grid methods (Nobile et al. 2008; Wu et al. 2021). Function expansion methods, such as polynomial chaos expansion (Bhattacharyya 2022, 2020, 2023; Jacquelin et al. 2019; Shao et al. 2017; Guo et al. 2019), introduce orthogonal polynomials to construct efficient surrogate models of the response function. Local expansion methods (Hu et al. 2021; Breitung 1984) require a first- or second-order Taylor expansion of the response function at the reference

points to efficiently compute the mean and variance. In addition, some PDF approximation methods have been proposed based on the statistical moments of the response function. They can be divided into five categories: Johnson systems (Trenkler 1994), Pearson family distributions (Pearson and I.X. 1916), saddlepoint approximation methods (Du 2007), generalized lambda distributions (Asquith 2007), and maximum entropy methods (Livesey and Brochon 1987).

In the above uncertainty propagation analysis, random variables are mainly considered as the unimodal distributions, such as normal, uniform, and Weibull distributions. However, random variables may follow multimodal distributions in engineering problems. For example, the fatigue lifetimes of safety cut specimens in aircraft structure follow a bimodal lognormal distribution after repair (Zeng et al. 2020). In long-term stress monitoring of steel bridges, the stress distribution follows a multimodal distribution (Ni et al. 2010). In the reliability optimization design, the unimodal distribution neglects the features of the multimodal distribution, which leads to insufficient accuracy. In areas with strict reliability requirements, such as the nuclear industry and the aerospace industry, insufficient accuracy can lead to serious disasters. Therefore, it is essential to develop efficient uncertainty propagation methods for multimodal distributions. There has been a small amount of research work on multimodal distribution problems. In terms of computational accuracy, sampling-based methods have been able to achieve satisfactory computational accuracy. However, they are widely known to be computationally demanding. As a result, they are difficult to apply to engineering problems involving complex simulation models. In terms of computational efficiency, moment-based methods have been developed. Du (Hu and Du 2018) introduced a first-order approximation method for bimodal distributions. The saddlepoint approximation method is used to obtain the reliability analysis results. Chen (Li et al. 2021) proposed a novel direct probability integration method (DPIM), which can be used to calculate the response function's PDF involved multimodal distributions. Zhang (Zhang et al. 2019) proposed a multimodal uncertainty propagation method based on univariate dimension reduction method (UDRM). In this method, UDRM is used to compute higher-order statistical moments. The PDF of the response function is computed using an adaptive framework based on the maximum entropy method. These methods are computationally efficient compared to sampling-based methods, but they may fail to provide satisfactory accuracy and efficiency when the response function is deeply nonlinear or complex. Thus, it is relatively difficult to consider both computational efficiency and accuracy at present.

This study presents a multimodal uncertainty propagation method that takes into account both computational efficiency and accuracy. Unimodal decomposition strategy and arbitrary polynomial chaos expansion improve the computational accuracy while ensuring computational efficiency. The study is organized as follows: In Sect. 2, the probability density function of multimodal random variables is established. In Sect. 3, elements are constructed where input random variables are unimodal distributions. In Sect. 4, the PDF of the response function in each element is computed and then the PDF of the response function in the complete probability space is obtained. In Sect. 5, the computational efficiency and accuracy of the proposed method are demonstrated by examples.

2 Uncertainty modeling of input multimodal random variables

Gaussian mixture model (GMM) can be used to determine the probability density function of the multimodal random variable X , which is expressed as follows (Figueiredo and Jain 2002):

$$f(x|\Theta) = \sum_{i=1}^N \omega_i \varphi(x|\theta_i) \tag{1}$$

where N is the number of Gaussian components, which can be obtained by direct observation or integral square difference (ISD) (Valverde et al. 2012); $\Theta = (\omega_1, \theta_1, \omega_2, \theta_2, \dots, \omega_N, \theta_N)$ is the parameter set of GMM; $\theta_i = (\mu_i, \sigma_i^2)$ represents the mean and variance at the i th Gaussian component; ω_i and $\varphi(x|\theta_i)$ denote the coefficient and probability density function at the i th Gaussian component, respectively. ω_i also satisfies $\omega_i \geq 0$ and $\sum_{i=1}^N \omega_i = 1$. A Gaussian mixture model of a multimodal distribution with four components is shown in Fig. 1.

Therefore, the parameter set Θ is required to be computed and applied to obtain the probability density function of X . Maximum likelihood estimation is a widely used method for parameter estimation. A sample set $s = \{s_1, s_2, \dots, s_h\}$ is obtained, where a latent variable set $\gamma = \{\gamma_1, \gamma_2, \dots, \gamma_N\}$ is introduced for each sample. $\gamma_i = 1$ denotes the sample located at the i th Gaussian component and the probability of the sample being located at this Gaussian component can be written as follows:

$$p(\gamma_i = 1) = \omega_i \tag{2}$$

Hence, the probability of the sample s_j can be expressed as follows:

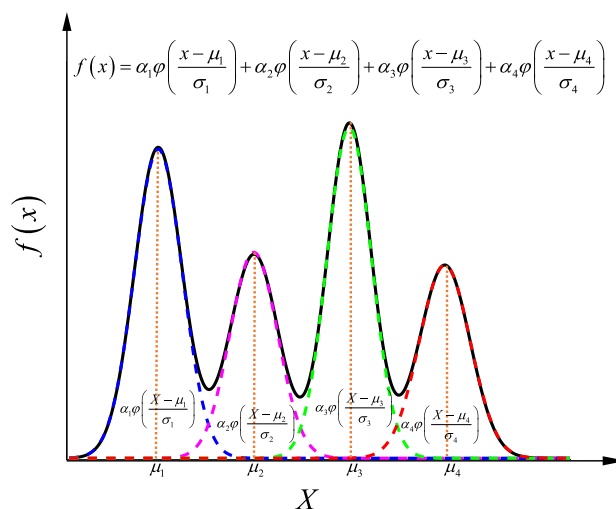


Fig. 1 Gaussian mixture model of multimodal distribution with four components

$$p(s_j) = \sum_{i=1}^N p(\gamma_i) p(s_j|\gamma_i) = \sum_{i=1}^N \omega_i \varphi(s_j|\theta_i) \tag{3}$$

The logarithmic form of the joint probability density function for each sample is considered as a log-likelihood function:

$$\log L(\Theta) = \log \left(\prod_{j=1}^h \sum_{i=1}^N \omega_i \varphi(s_j|\theta_i) \right) = \sum_{j=1}^h \log \sum_{i=1}^N \omega_i \varphi(s_j|\theta_i) \tag{4}$$

Set the derivation of Eq. (4) equal to 0, and the parameter set Θ is calculated as follows:

$$\hat{\Theta} = \arg \max_{\Theta} \{ \log L(\Theta) \} \tag{5}$$

In fact, it is difficult to directly calculate Θ based on the formula (5). Therefore, the expectation–maximization algorithm (Castillo-Barnes et al. 2020) is often used to search for the local maximum of $\log L(\Theta)$.

3 Unimodal decomposition strategy

In early research, a decomposition method is proposed for multimodal random variables (Nouy 2010). This method decomposed a partition of $[0, 1)$ into multiple discrete intervals and constructed the desired partitions of a multimodal random variable based on them. The purpose of the unimodal decomposition strategy is also to transform multimodal random variables into a set of unimodal random variables. The difference is that the method is based on a direct decomposition of multimodal random variables in terms of

minimum points, and it is aimed at the multidimensional multimodal random variables. Three steps are involved in unimodal decomposition strategy: (i) determining the division points of the multimodal random variables, (ii) decomposing multimodal random variables by division points and constructing unimodal elements, and (iii) computing the response function's PDF.

Division points can be used in the decomposition of multimodal random variables, and the computational accuracy of the division points can affect the effect of the decomposition. The division point is defined at the lowest point between two neighboring components of the multimodal distribution. The probability density functions of the multimodal random variables are treated as objective functions and the division points are considered as local minima of them. According to the mathematical properties of local minima, the points around the division points satisfy the following conditions:

$$\nabla f(a) < 0, \nabla f(b) > 0 \tag{6}$$

where ∇f is the derivation of the objective function. a and b are the points to the left and right of the division point, respectively. The search intervals of the minimum points are determined based on Eq. (6), and then the local minimum point of each interval is calculated by the univariate optimization methods. The division points of the multimodal random variables are used to define disjoint division intervals. Each multimodal random variable X can be decomposed into a set of random variables, where each random variable follows a unimodal distribution. The decomposition procedure for a multimodal distribution with four components is shown in Fig. 2.

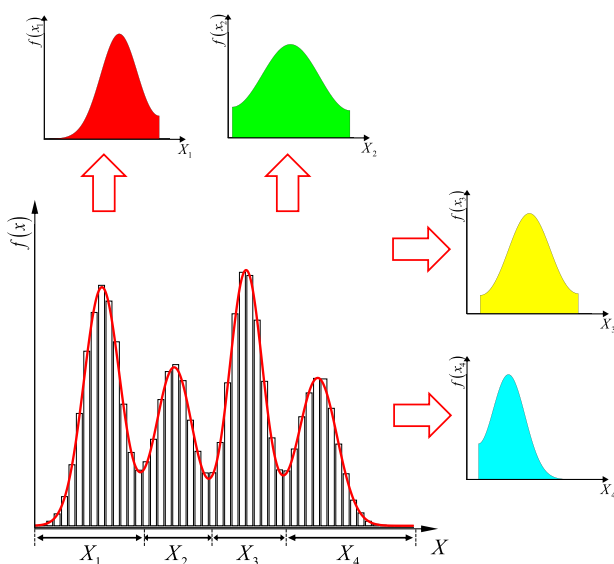


Fig. 2 The decomposition of multimodal distribution

This is essential for reconstructing uncertainty propagation problems after decomposition of multimodal random variables. All sets of random variables are chosen to construct elements B_k , each of which contains various independent random variables. The elements are disjoint and satisfy the following conditions:

$$\begin{cases} B_k = [X_{k,1}, X_{k,2}, \dots, X_{k,d}] \\ B = \bigcup_k^{N_1} B_k \\ B_{k_1} \cap B_{k_2} = \phi \quad \text{if } k_1 \neq k_2 \end{cases} \tag{7}$$

where $X_{k,i}$ is a random variable in the i th set and an element B_k . d is the number of independent multimodal random variables. N_1 is the number of elements. Thus, N_1 disjoint elements are constructed based on the decomposition of the multimodal distribution. The construction of the elements in the two-dimensional probability space is described using Fig. 3.

The above method transforms the uncertainty propagation for multimodal distributions into a set of uncertainty propagation for unimodal distributions. In this way, elements are treated as multidimensional uncertainty propagation problems and PDFs of various response functions are included. The PDF of the response function $f(y)$, for a multimodal distribution, can be determined based on the elements. The statistical moments of the response function m_i are decomposed into various statistical moments in the elements and the procedure can be stated as follows:

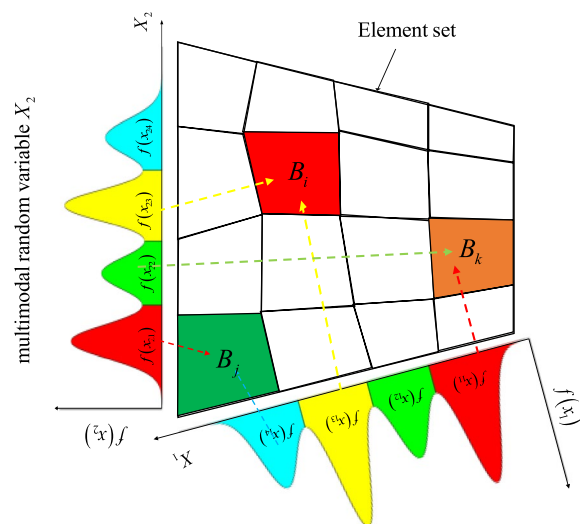


Fig. 3 The construction of elements in a two-dimensional probability space

$$\begin{aligned}
 m_i &= \int_{\mathbf{X}} g(\mathbf{x})f_{\mathbf{X}}(\mathbf{x})d\mathbf{x} = \sum_{k=1}^{N_1} P(B_k) \int_{X_k} g(\mathbf{x}_k)f_{X_k}(\mathbf{x}_k)d\mathbf{x}_k \\
 &= \sum_{k=1}^{N_1} P(B_k)m_{k,i}
 \end{aligned}
 \tag{8}$$

where $P(B_k)$ is the probability of element B_k . $\mathbf{X} = (X_1, X_2, \dots, X_d)$ denotes the vector of d independent multimodal random variables. $m_{k,i}$ is the i th-order statistical moment in element B_k . The PDF of the response function in each element based on $m_{k,i}$ is estimated using the maximum entropy method. Hence, $f(y)$ is decomposed as follows:

$$f(y) = \sum_{k=1}^{N_1} P(B_k)f_k(y)
 \tag{9}$$

where $f_k(y)$ is the PDF of the response function in element B_k . Let $F_k(y) = P(B_k)f_k(y)$, and Eq. (9) can be rewritten as follows:

$$f(y) = \sum_{k=1}^{N_1} F_k(y)
 \tag{10}$$

The uncertainty propagation based on the unimodal decomposition strategy is shown in Fig. 4. The random variables follow unimodal distributions in each element, and then $f_k(y)$ can be estimated from the first 4th-order statistical moments. Specific computation methods are shown in Sect. 4. Thus, it can be found that the first 4th-order statistical moments are required to determine $f(y)$ in this method.

Equation (9) indicates that $P(B_k)$ are also required to be determined and the computation process is shown as follows: First, MCS is used to produce n samples and they can be divided into various elements. Second, an indicator function I_{B_k} , which is used to determine whether the samples belong to the element B_k , is initially defined for them.

$$I_{B_k} = \begin{cases} 1 & \text{if } \mathbf{x}_{B_k} \in B_k \\ 0 & \text{otherwise} \end{cases}
 \tag{11}$$

It can be found that $I_{B_k} = 1$ indicates that the sample is located at the element B_k . The distribution ratios of the samples are considered as $P(B_k)$, and they can be expressed as follows:

$$P(B_k) = P(I_{B_k} = 1) = \frac{n_k}{n}
 \tag{12}$$

where n_k is the number of samples located at element B_k .

4 Uncertainty propagation in unimodal elements

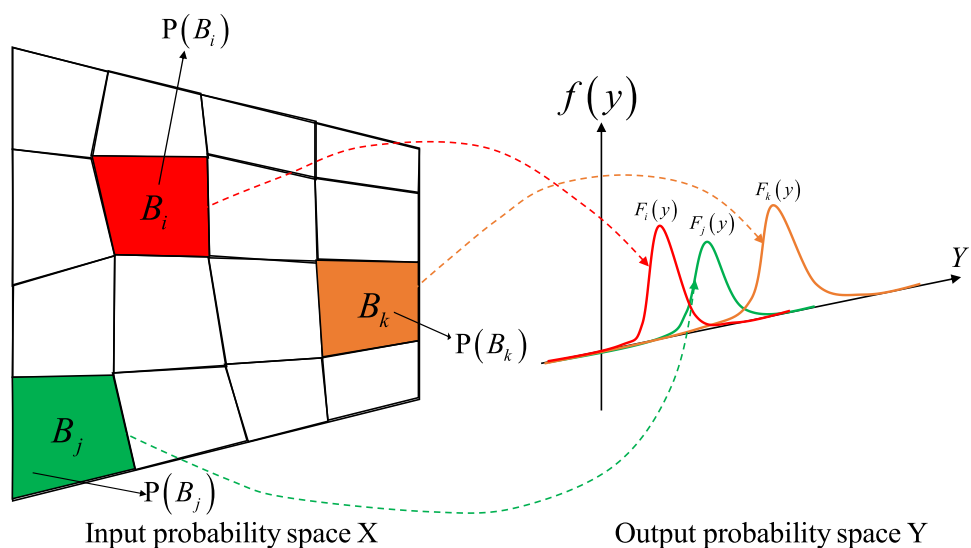
In this section, uncertainty propagation is performed for unimodal random variables in each element, where the arbitrary polynomial chaos expansion and maximum entropy method are involved.

4.1 Calculating the statistical moments of the response function

Based on the random variables X_k in the elements, the surrogate model of response function $Y=g(\mathbf{X}_k)$ can be constructed by polynomial chaos expansion (PCE) (Sachdeva et al. 2006):

$$\hat{g}(\mathbf{X}_k) \approx \sum_{i=0}^P \alpha_{k,i} \Phi_i(\mathbf{X}_k)
 \tag{13}$$

Fig. 4 The uncertainty propagation based on unimodal decomposition strategy



where p is the number of truncated expansion terms. α_i denotes a polynomial coefficient. $\Phi_i(\mathbf{X}_k)$ stands for the multivariable PCE basis, which can be expressed as follows:

$$\Phi_i(\mathbf{X}_k) = \prod_{j=1}^d \phi_{i_j}(X_{k,j}) \tag{14}$$

where $\phi_{i_j}(X_{k,j})$ is the one-dimensional orthogonal polynomial chaos basis of the random variable $X_{k,j}$. Therefore, $\alpha_{k,i}$ and $\phi_{i_j}(X_{k,j})$ are required to be computed to determine the surrogate model $\hat{g}(\mathbf{X}_k)$.

A moment-based analysis (Oladyshkin and Nowak 2012) is used to construct a multivariable PCE basis for arbitrary distributions. The k th-order one-dimensional orthogonal polynomial chaos basis $\phi_{i_j}^{(k)}(X_{k,j})$ can be defined as follows:

$$\phi_{i_j}^{(k)}(X_{k,j}) = \sum_{m=0}^K \beta_m^{(k)} X_{k,j}^m \tag{15}$$

where $\beta_m^{(k)}$ are unknown parameters. $X_{k,j}^m$ are m th power of $X_{k,j}$. $\phi_{i_j}^{(K_1)}(X_{k,j})$ and $\phi_{i_j}^{(K_2)}(X_{k,j})$ satisfy the following requirements:

$$\begin{aligned} & \langle \phi_{i_j}^{(K_1)}(X_{k,j}), \phi_{i_j}^{(K_2)}(X_{k,j}) \rangle \\ &= \int_{X_{k,j}} \phi_{i_j}^{(K_1)}(x_{k,j}) \phi_{i_j}^{(K_2)}(x_{k,j}) f(x_{k,j}) dx_{k,j} \tag{16} \\ &= 0, \forall K_1 \neq K_2 \end{aligned}$$

The K th-order statistical moment of a random variable $X_{k,j}$ can be expressed as follows:

$$\mu_K = \int_{X_{k,j}} x_{k,j}^K f(x_{k,j}) dx_{k,j} \tag{17}$$

Equation (16) is transformed into matrix form based on Eq. (15) and Eq. (17):

$$\begin{bmatrix} \mu_0 & \mu_1 & \dots & \mu_K \\ \mu_1 & \mu_2 & \dots & \mu_{K+1} \\ \vdots & \vdots & \vdots & \vdots \\ \mu_{K-1} & \mu_K & \dots & \mu_{2K-1} \\ 0 & 0 & \dots & 1 \end{bmatrix} \begin{bmatrix} \beta_0^{(K)} \\ \beta_1^{(K)} \\ \vdots \\ \beta_{K-1}^{(K)} \\ \beta_K^{(K)} \end{bmatrix} = \begin{bmatrix} 0 \\ 0 \\ \vdots \\ 0 \\ 1 \end{bmatrix} \tag{18}$$

$\beta_i^{(K)}$ is determined based on Eq. (18) and $\Phi_i(\mathbf{X}_k)$ can be constructed based on Eq. (14).

The polynomial coefficients $\alpha_{k,i}$ can be written as follows:

$$\alpha_{k,i} = \int_{X_k} g(\mathbf{x}_k) \Phi_i(\mathbf{x}_k) f(\mathbf{x}_k) d\mathbf{x}_k \tag{19}$$

Equation (19) is a multivariate integral problem and sparse grid method is applied to calculate the multivariate integral in this study. It is necessary to determine the integration points and weights of the random variables. The Hankle positive definite matrix \mathbf{H} is built from the statistical moments of the random variables $\mu_K, K = 1, 2, \dots, 2p_1$. The upper triangular matrix \mathbf{C} is constructed from the Cholesky decomposition $\mathbf{H} = \mathbf{C}^T \mathbf{C}$:

$$\mathbf{C} = \begin{bmatrix} c_{1,1} & c_{1,2} & \dots & c_{1,p_1+1} \\ & c_{2,2} & \dots & c_{2,p_1+1} \\ & & \ddots & \vdots \\ & & & c_{p_1+1,p_1+1} \end{bmatrix} \tag{20}$$

$\phi_{i_j}^{(K)}(X_{k,j}), K = 1, 2, \dots, p_1$ (Ahlfeld et al. 2016) satisfy the following equation:

$$X_{k,j} \phi_{i_j}^{(K)}(X_{k,j}) = b_{K-1} \phi_{i_j}^{(K-2)}(X_{k,j}) + a_{k,K} \phi_{i_j}^{(K-1)}(X_{k,j}) + b_K \phi_{i_j}^{(K-1)}(X_{k,j}) \tag{21}$$

where the parameters a_K and b_K are expressed as:

$$a_K = \frac{c_{K,K+1}}{c_{K,K}} - \frac{c_{K-1,K}}{c_{K-1,K-1}}, b_K = \frac{c_{K+1,K+1}}{c_{K,K}}, c_{0,0} = 1, c_{0,1} = 0 \tag{22}$$

Equation (21) can be rewritten as a positive definite symmetric tridiagonal Jacobi matrix J :

$$J = \begin{bmatrix} a_1 & b_1 & & & \\ b_1 & a_2 & b_2 & & \\ & b_2 & a_3 & b_3 & \\ & & \ddots & \ddots & \ddots \\ & & & b_{p_1-2} & a_{p_1-1} & b_{p_1-1} \\ & & & & b_{p_1-1} & a_{p_1} \end{bmatrix} \tag{23}$$

The integration points and weights of the random variables are determined by the eigenvalues and the corresponding normalized eigenvectors of the matrix J , respectively. Special tensor product operations (Smolyak 1963) are then performed to determine the configuration points and weights used to compute the polynomial coefficients. The 1st-order statistical moment can be determined as follows:

$$E[g(\mathbf{X}_k)] = \alpha_{k,0} \tag{24}$$

where α_0 is the first polynomial coefficients. The l th-order statistical moment $E[g^l(\mathbf{X}_k)]$ can also be calculated using this equation. Defining formula as follows:

$$G(\mathbf{X}_k) = g^l(\mathbf{X}_k) \tag{25}$$

Thus, the l th-order statistical moment of $Y = g(\mathbf{X}_k)$ is transformed into the 1st-order statistical moment of $Y = G(\mathbf{X}_k)$.

4.2 Computing the probability density function of the response function

Based on the statistical moments, the PDF of the response function in the elements is computed using the maximum entropy method. The first 4th-order statistical moments are applied to estimate the probability density function of the random variable. The entropy value indicates the estimation accuracy of the probability density function. In order to estimate a more accurate probability density function, the response function Y_k needs to be normalized. The constrained optimization problem (Sobczyk and Trzebicki 1999) can be written as follows:

$$\begin{cases} \max_{f_k} S(f_k) \\ \text{s.t.} \int_{Y_k} \left(\frac{y - \mu_{Y_k}}{\sigma_{Y_k}} \right)^i f_k(y) dy = m'_{k,i}, i = 0, 1, \dots, 4 \end{cases} \quad (26)$$

where μ_{Y_k} and σ_{Y_k} denote the mean and variance of the response function in element B_k , respectively. $f_k(y)$ represents the estimated PDF of the response function. $S(f_k)$ is the entropy value of $f_k(y)$:

$$S(f_k) = \int_{Y_k} f_k(y) \ln(f_k(y)) dy \quad (27)$$

$m'_{k,i}$ indicates a non-standard central moment that is determined by the original statistical moment $m_{k,i}$:

$$m'_{k,i} = \frac{1}{c!} \left[\sum_{j=1}^{i+1} (-1)^{j+1} C_i^j (m_1)^{j-1} m_{i-j+1} \right], i = 0, 1, \dots, 4 \quad (28)$$

where $C_i^j = \binom{i}{j-1}$ is binomial coefficient. $m_{k,0}$ represents the 0th-order statistical moment in element B_k . c denotes the proportional factor of $m'_{k,i}$. The response function's PDF can be estimated by the constrained optimization problem in Eq. (26). After obtaining the response function's PDF $f_k(y)$ in all elements, the response function's PDF $f(y)$ is calculated by using Eq. (9) and Eq. (12).

4.3 Numerical procedure

In the proposed method, elements are constructed and the probabilities of elements are computed in Sect. 3. The PDF of the response function in the elements is then computed in Sect. 4. The PDF of the response function for the multimodal distribution is determined based on the probabilities of the elements and the PDF of the response function in the elements. The numerical procedure of the proposed method is

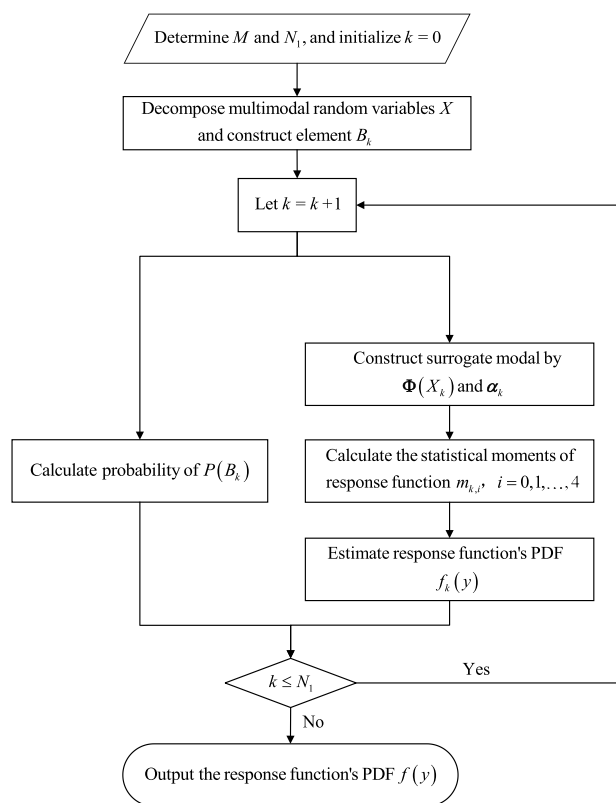
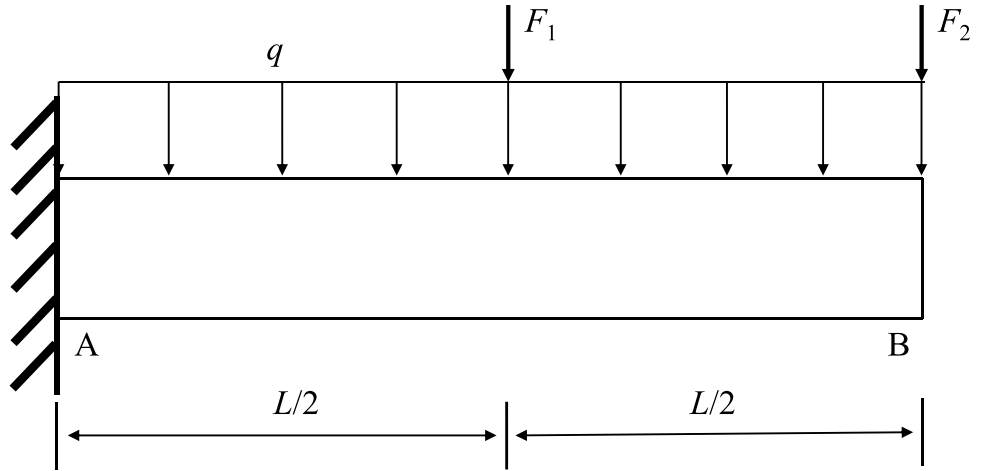


Fig. 5 Flow chart of the proposed method

illustrated in Fig. 5, and the detailed procedure is presented below:

- Step 1 Determine the number of division points M , the total number of elements N_1 and initialize the current element number $k = 0$.
- Step 2 Decompose the multimodal random variables X based on the division points and obtain the unimodal random vectors $X = [X_1, X_2, \dots, X_{M+1}]$.
- Step 3 Construct elements B_k based on Eq. (7).
- Step 4 Let $k = k + 1$.
- Step 5 Calculate the probability of the current element $P(B_k)$ by samples using Eq. (12).
- Step 6 Calculate orthogonal polynomial chaos basis $\Phi(X_k)$ using Eq. (14) and polynomial coefficient α_k using Eq. (19) in the current element.
- Step 7 Calculate the statistical moments of the response function $m_{k,i}, i = 0, 1, \dots, 4$ in the current element using Eq. (24) and Eq. (25).

Fig. 6 Circular section column model (Fan et al. 2016)



- Step 8 Calculate the response function’s PDF $f_k(y)$ in the current element using Eq. (26) based on statistical moments $m_{k,i}$.
- Step 9 If $k \leq N_1$, repeat step 2 to step 8. Otherwise, go to step 9.
- Step 10 Output the response function’s PDF $f(y)$ for the multimodal distribution using Eq. (9).

5 Numerical examples

In this section, three examples are used to verify the computational accuracy and efficiency of the proposed method, and MCS is used as a validation method to verify the computational accuracy and efficiency. The method UDRM (Zhang et al. 2019) has the requirement of computing higher-order statistical moments. Thus, it is used as a comparison method. The relative error (RE) ϵ_{RE} and Kullback–Leibler divergence (KLD) ϵ_{KL} are used for accuracy analysis, where RE is defined as:

$$\epsilon_{RE} = \frac{|V - V_{MCS}|}{V_{MCS}} \times 100\% \tag{29}$$

where V_{MCS} is the solution at a certain value of the CDF computed by MCS; V is a solution computed by other methods.

ϵ_{KL} is defined as:

$$\epsilon_{KL}(P||Q) = \sum_{x \in \chi} P(x) \log \left(\frac{Q(x)}{P(x)} \right) \tag{30}$$

where P and Q are the PDFs obtained by MCS and other methods, respectively; χ is probability space.

5.1 Linear elastic cantilever beam force problem

A linear elastic cantilever beam is loaded with one distributed load and two concentrated loads as illustrated in Fig. 6. In this example, the displacement PDF at point B is determined. The displacement at point B is denoted as:

$$\Delta_B = f(q, F_1, F_2, E, I, L) = \frac{qL^4}{8EI} + \frac{5F_1L^3}{48EI} + \frac{F_2L^3}{3EI} \tag{31}$$

where q is distributed load. F_1 and F_2 represent various concentrated loads. E , I and L denote the elastic modulus of material, the moment of inertia of beam section and the length of linear elastic cantilever beam, respectively.

F_2 , I , and L are determined parameters that $F_2=100 \times 10^3N$, $L=3000mm$ and $I= 5.3594 \times 10^8mm^4$. q , F_1 , and E are multimodal random variables. Distributional properties of random variables are presented by a large amount of observational data. Therefore, a GMM with four Gaussian components is used to construct the probability density function of multimodal random variables, as illustrated in Fig. 7. The distribution parameters of the multimodal random variables are listed in Table 1.

Based on the multimodal random variables q , F_1 , and E , the displacement PDF at point B is computed using the proposed method. The decomposition of the multimodal random variables into multiple random variables based on the division points is illustrated in Fig. 8.

Multimodal random variables are decomposed into four random variables. Therefore, three sets of random variables are obtained. The random variables are chosen to form the elements, and a total of 64 elements are constructed in this example. MCS is continuously used to verify the accuracy of the proposed method based on a large number of samples (1×10^6), which are generated using the probability density functions of the multimodal random variables q , F_1 , and E .

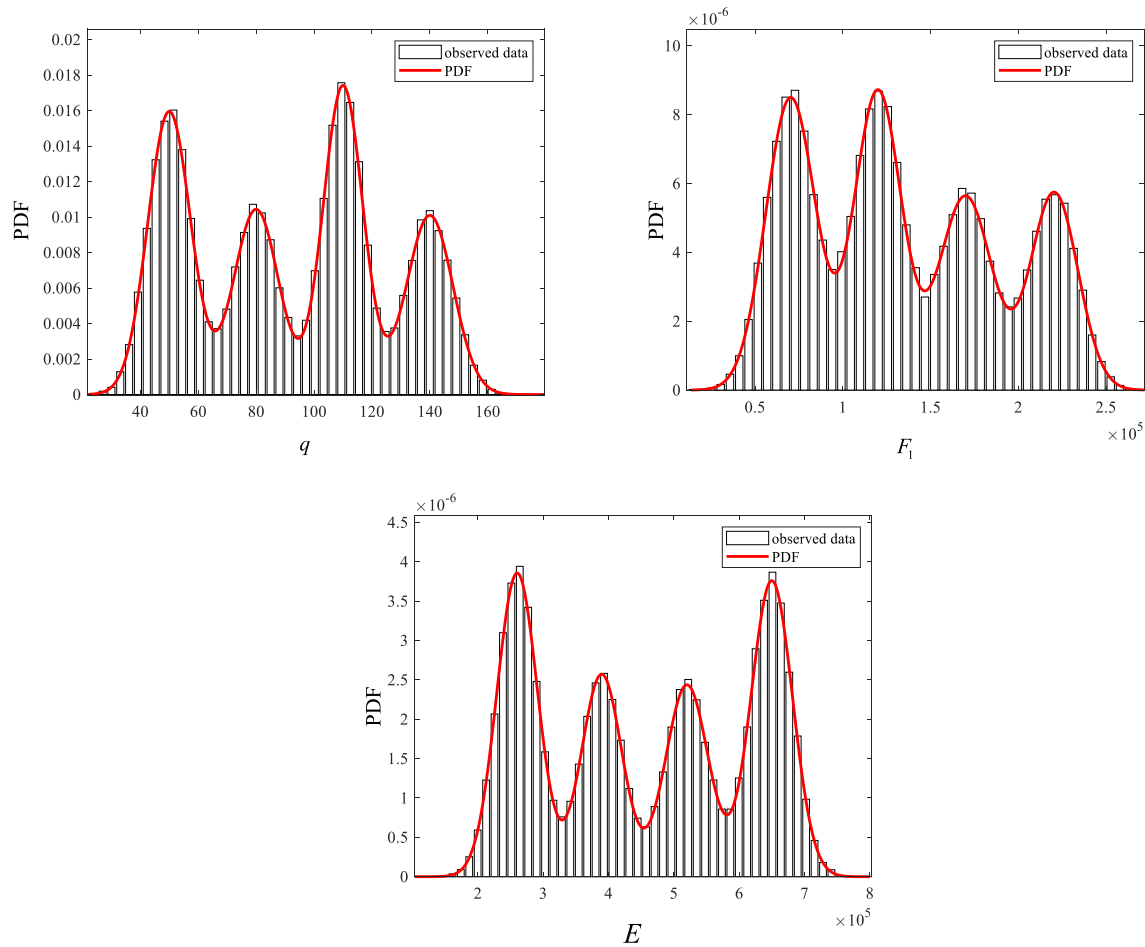


Fig. 7 Distribution of multimodal random variables

Table 1 Distribution parameters of multimodal random variables

Random variables	Coefficients	Mean values	Standard deviations
q	(0.3, 0.2, 0.3, 0.2)	(50, 80, 110, 140)	(7.5, 7.5, 7, 8)
F_1	(0.3, 0.3, 0.2, 0.2)	(7×10^4 , 12×10^4 , 17×10^4 , 22×10^4)	(14×10^3 , 14×10^3 , 14×10^3 , 14×10^3)
E	(0.3, 0.2, 0.2, 0.3)	(26×10^4 , 39×10^4 , 52×10^4 , 65×10^4)	(312×10^2 , 312×10^2 , 322×10^2 , 318×10^2)

The results of uncertainty propagation are determined by the proposed method, UDRM, and MCS. They are illustrated in Fig. 9. The PDF and CDF obtained by the proposed method are very close to MCS. For illustration, the CDF values and RE of the proposed method, UDRM, are listed in Table 2, where four locations are considered. The frequency histograms of the response functions constructed by MCS with UDRM and the proposed method are shown in Fig. 10. Then, ϵ_{KL} can be calculated by Eq. (30).

It can be found that the proposed method obtains better computational accuracy at these locations. The RE of the proposed method is considerably lower than that of UDRM. The largest RE of the proposed method and the UDRM are both located at $y=7.5$, with values of 0.0297% and 8.5706%, respectively. The KLD of MCS and UDRM is 0.0441. The KLD of MCS and the proposed method is smaller, with a value of 0.0013. Hence, the proposed method has the best computational accuracy among them. Computation of

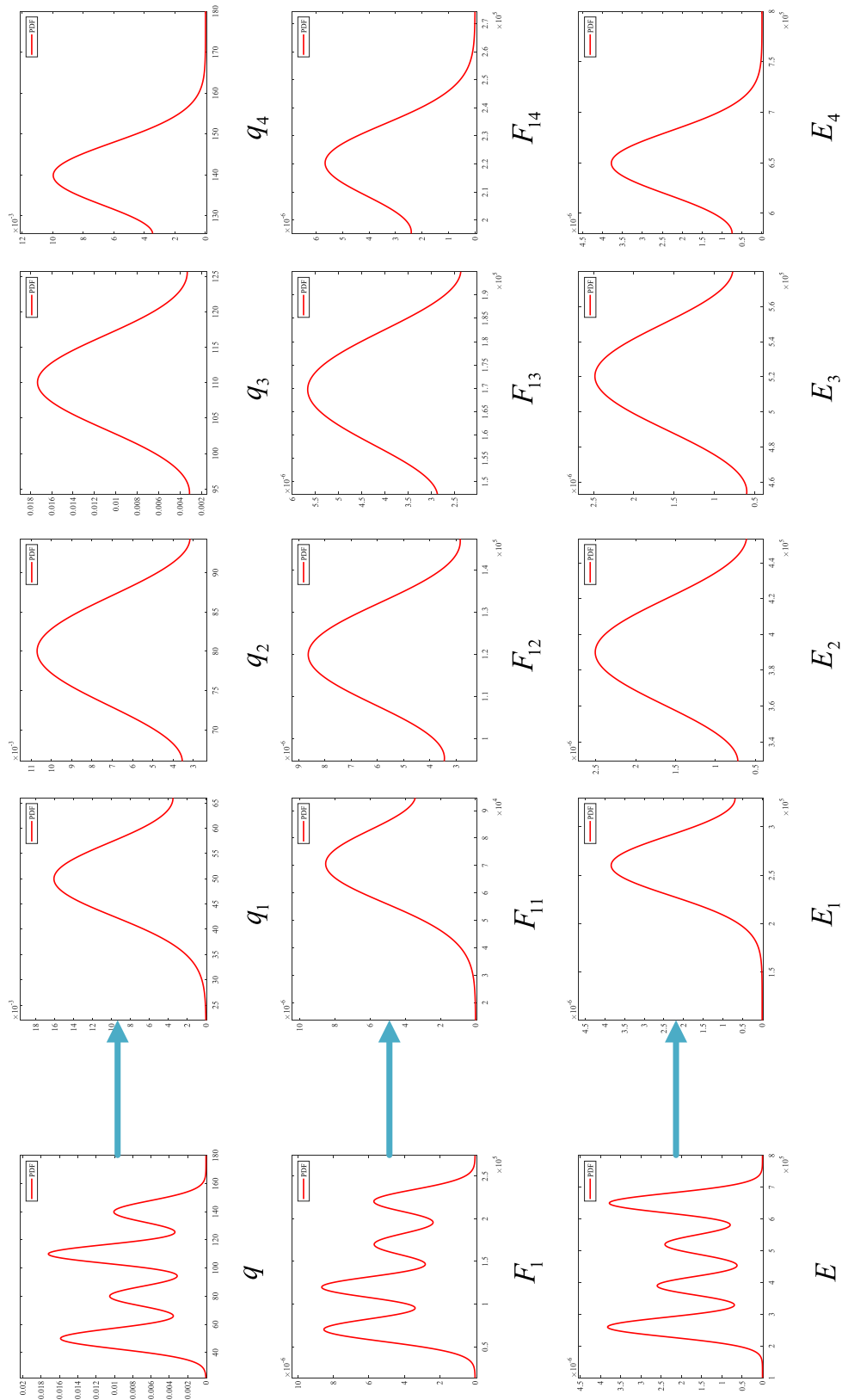


Fig. 8 Decomposition of multimodal random variables

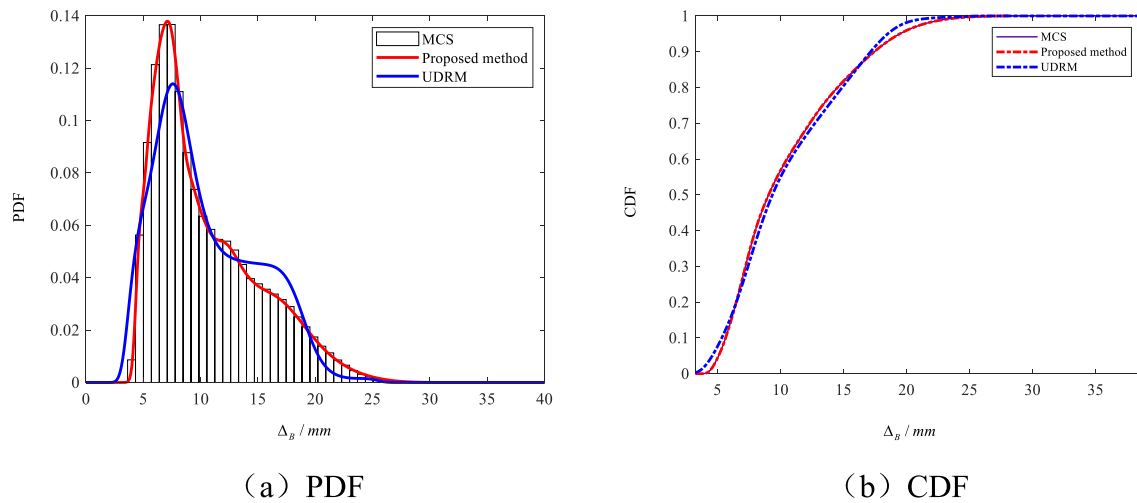


Fig. 9 The uncertainty propagation results of proposed method, UDRM, and MCS

Table 2 CDF values and RE of different locations

	$y = 7.5(\text{RE, \%})$	$y = 10(\text{RE, \%})$	$y = 12.5(\text{RE, \%})$	$y = 15(\text{RE, \%})$
Proposed method	0.3373(0.0297)	0.5679(0.0176)	0.7091(0.0141)	0.8179(0.0037)
UDRM	0.3083(8.5706)	0.5491(3.2934)	0.6887(2.8906)	0.8046(1.6225)

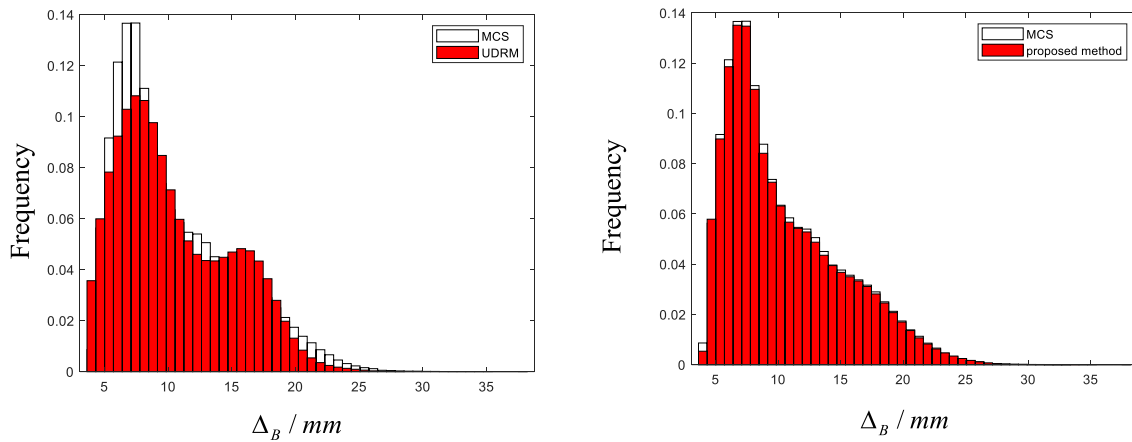


Fig. 10 Frequency histograms of MCS with different methods

higher-order statistical moments not only increases the computational error, but also increases the computational complexity. The proposed method requires the first 4th-order statistical moments, while UDRM requires the first 12th-order statistical moments to construct the PDF of the response function. In addition, UDRM needs to call the response function to calculate 31 times, the proposed method needs to call the response function to calculate 1792 times and MCS needs to call the response function to calculate 1×10^6 times. Therefore, UDRM and the proposed method are more computationally efficient than MCS. However, the proposed

method has the best performance among them, considering both computational accuracy and efficiency.

5.2 The uncertainty propagation problem of RV reducer

RV reducer are an integral part of industrial robots and are widely used in the industrial robotics field. For light industrial robots, the RV reducer only considers the first to the fourth joint. However, for heavy industrial robots, all joints

Fig. 11 RV reducer structure diagram (Yang et al. 2021)

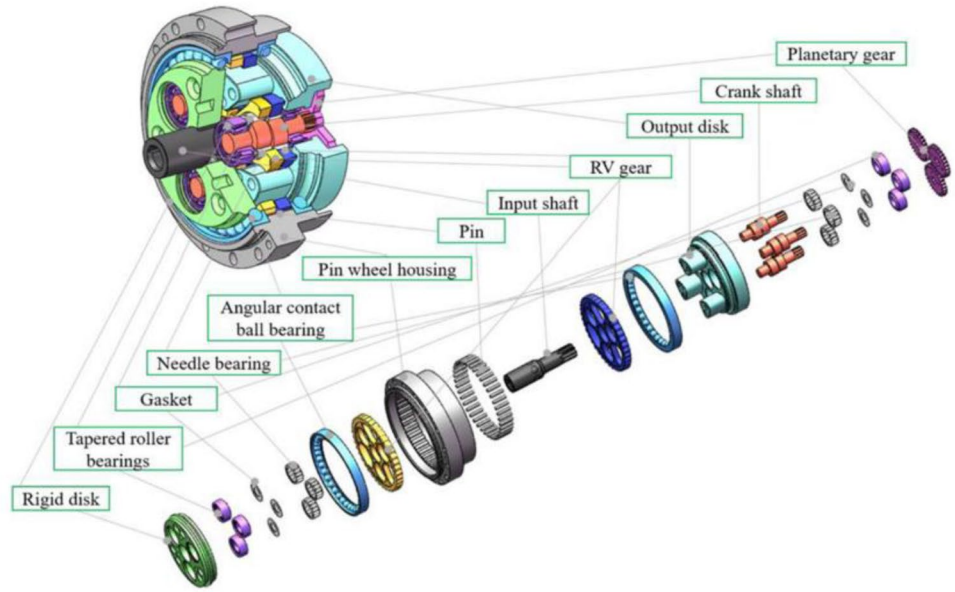


Table 3 Distribution parameters of random variables

Random variables	Coefficients	Mean values	Standard deviations
d_1	(0.5, 0.5)	(1.65, 2.61)	(0.16, 0.18)
d_2	(0.4, 0.6)	(12.5, 17.9)	(1.2, 1.3)
d_3	(0.4, 0.6)	(49.4, 59.4)	(2.5, 2.5)
X_1	(0.6, 0.4)	(4.48, 5.31)	(0.15, 0.18)

of the RV reducer need to be considered. The mechanism of the RV reducer mainly includes the central gear with input shaft, planetary gear, crank shaft, RV gear, pin gear, pin wheel housing, tapered roller bearing, gasket, needle bearing, angular contact ball bearing and output mechanism. The structure diagram is illustrated in Fig. 11.

The gear teeth of the planetary gear are required to satisfy the contact fatigue strength of the tooth surface. Therefore, the response function of the contact fatigue strength of the planetary gear teeth is defined as follows:

$$Y = g(d, X) = 297.6064 \sqrt{\frac{7161.8144}{X_1 d_1 d_2} (d_2 + d_3)} - 1100 \tag{32}$$

where d_1, d_2, d_3 , and X_1 represent modulus, number of central gear, number of planetary gear, and width of planetary gear, respectively. Parameter d_1, d_2, d_3 , and X_1 are multimodal random variables. Distributional properties of random variables are presented by a large amount of observational data. Therefore, GMM with two Gaussian components is used to construct the probability density function of multimodal random variables. Distribution parameters of random variables d_1, d_2, d_3 , and X_1 are listed in Table 3.

Based on the probability density functions of the multimodal random variables d_1, d_2, d_3 , and X_1 , the proposed method is employed to compute the probability density function of the contact fatigue strength of the planetary gear tooth Y . Each multimodal random variable is decomposed into two random variables and four sets of random variables are constructed, as illustrated in Fig. 12. Thus, a total of 16 elements are determined in this example.

The computational accuracy of the statistical moments in the elements may change with the order of the polynomial P . The log RE of the statistical moments with the orders of the polynomial P are illustrated in Fig. 13. It follows that log RE is extremely large when $P = 1$. Then, the log RE becomes extremely small and remains stable when $P \geq 2$. Therefore, when $P=2$, the optimal computational accuracy can be achieved with the proposed method.

The results of uncertainty propagation are calculated using the proposed method, UDRM, and MCS and are illustrated in Fig. 14. It can be found that the PDF and CDF obtained by the proposed method are highly close to MCS, but the results obtained by UDRM are different from MCS. The CDF values and relative errors of the proposed method, UDRM, are listed in Table 4, where four locations are considered. The frequency histogram of the response function constructed by MCS with UDRM and the proposed method is shown in Fig. 15. Then, ϵ_{KL} can be calculated by formula (30).

The RE of the proposed method is less than 1% at these locations, with the smallest being 0.0729%. However, the RE of UDRM is considerably larger than that of the proposed method, with a minimum of 3.4575%. The KLD of MCS and UDRM is 0.0288. The KLD of MCS and the proposed method is smaller, with a value of 0.0018. Hence,

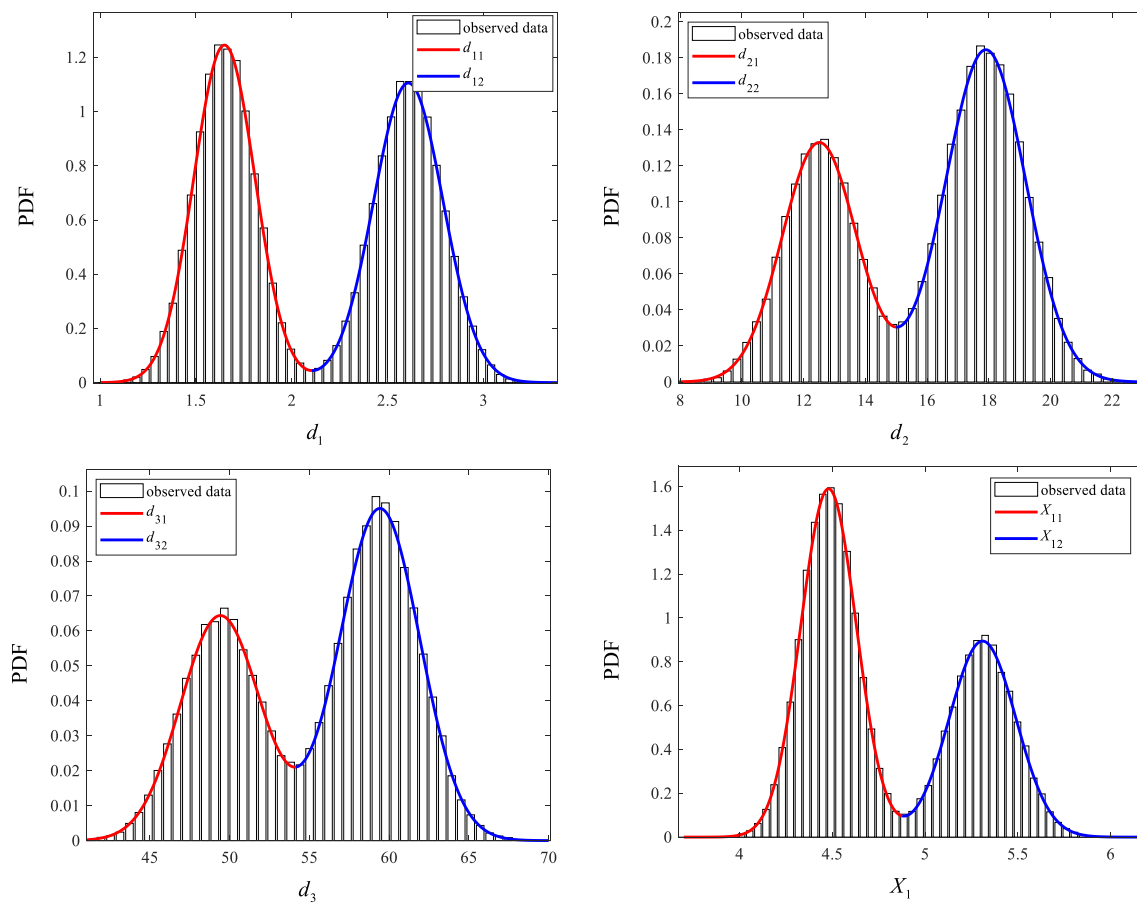


Fig. 12 The decomposition of multimodal random variables

the proposed method has the best computational accuracy among them. The proposed method and UDRM require the first 4th-order statistical moments and first 8th-order statistical moments to construct the PDF of the response function, respectively. Computing the statistical moments of the UDRM is more complicated than the proposed method. UDRM needs to call the response function to calculate 41 times to estimate the PDF, the proposed method needs to call the response function to calculate 720 times and MCS needs to call the response function to calculate 1×10^6 times to compute the PDF. The computational efficiency of the proposed method is lower than UDRM but higher than MCS. However, the proposed method requires fewer statistical moments. Therefore, the proposed method has the best performance among them, considering both computational accuracy and efficiency.

5.3 Vehicle collision problem

Lightweight design is employed in the vehicle industry and improves the energy consumption performance of the vehicle. However, a lightweight design may weaken the

vehicle’s crashworthiness. Therefore, collision analysis is used to verify crashworthiness. The structure diagram and simulation model of the vehicle are illustrated in Fig. 16. The failure analysis for high-speed frontal impact of a vehicle is performed at a speed of 56.4 km/h. In high-speed collisions, it is necessary to retain a relatively safe space to reduce passenger injuries. Hence, the intrusion of the marker points under the left back chair I_L is a highly valuable indicator.

The thickness of the front bumper X_1 , the inner plate of the anti-collision box X_2 , the outer plate of the anti-collision box X_3 , the inner plate of the front longitudinal beam X_4 , and the outer plate of the front longitudinal beam X_5 lead to a large influence on the intrusion of the marked point I_L , which mathematically can be expressed as follows:

$$I_L(\mathbf{X}) = g(X_1, X_2, X_3, X_4, X_5) \tag{33}$$

The response surface of the intrusion quantity for the landmark under the left back chair I_L is established by

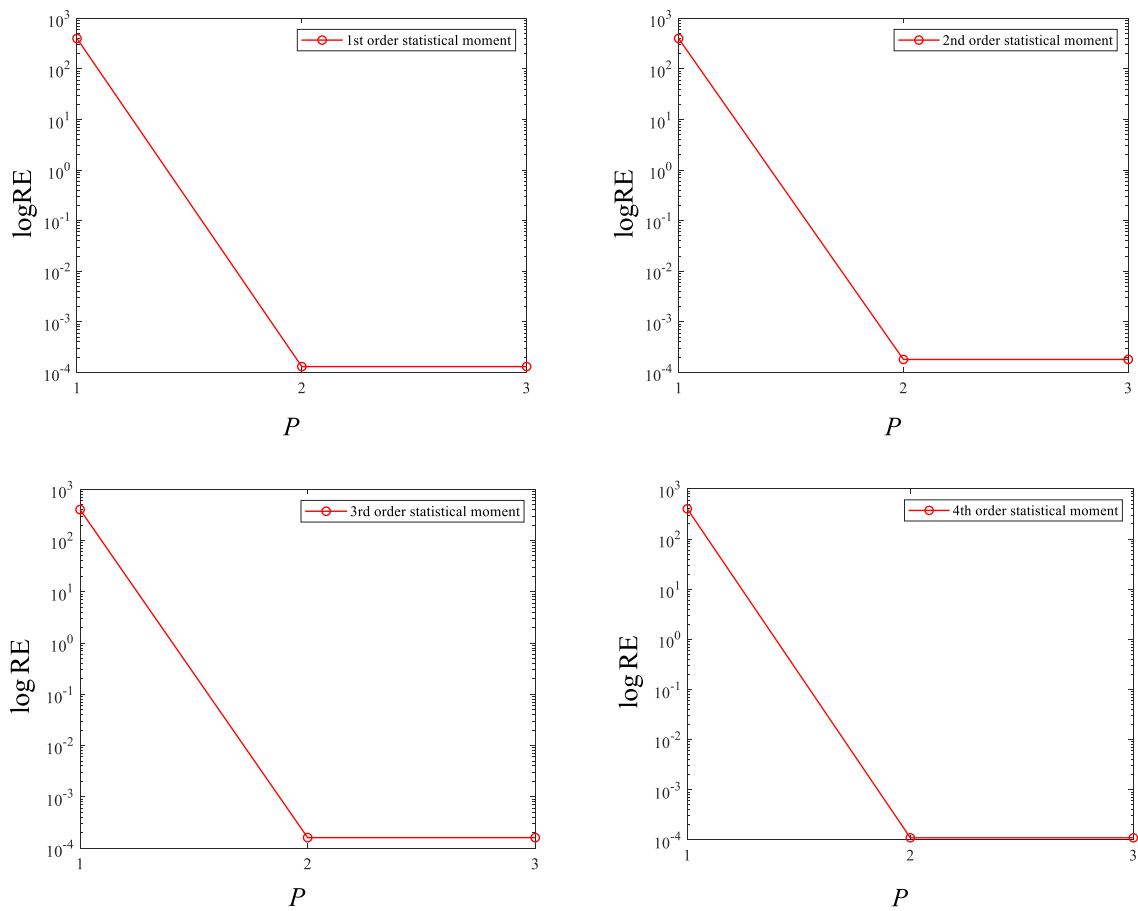


Fig. 13 The log RE with the orders of polynomial

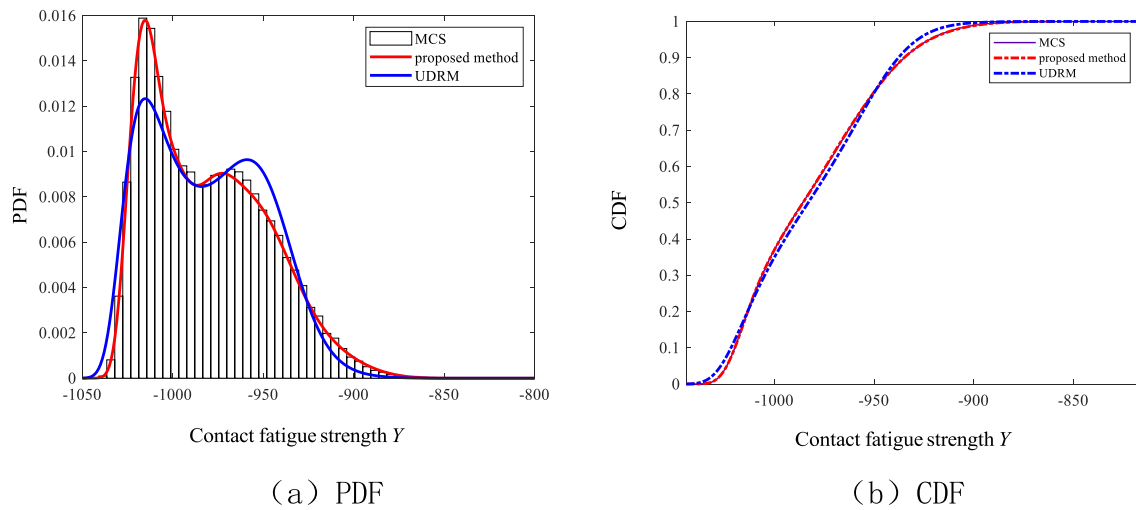


Fig. 14 The uncertainty propagation results of the proposed method, UDRM, and MCS

Table 4 CDF values and relative errors of different locations

	$y = -1000(\text{RE}, \%)$	$y = -990(\text{RE}, \%)$	$y = -980(\text{RE}, \%)$	$y = -970(\text{RE}, \%)$
Proposed method	0.3704(0.1886)	0.4632(0.2154)	0.5492(0.0729)	0.6389(0.4086)
UDRM	0.3499(5.7128)	0.4412(4.9548)	0.5262(4.1181)	0.6143(3.4575)

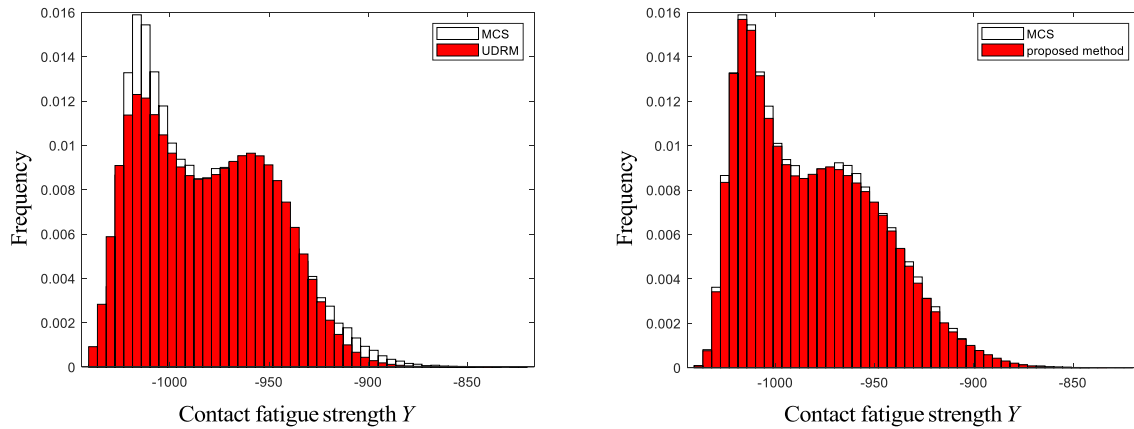
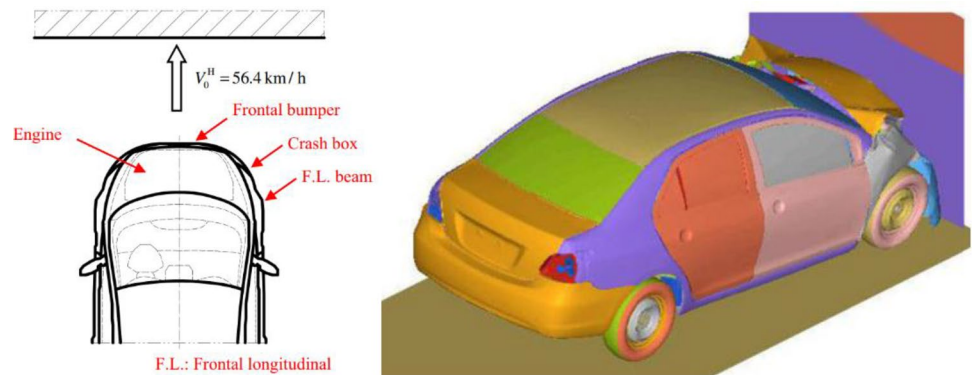


Fig. 15 Frequency histograms of MCS with different methods

Fig. 16 Structure diagram and simulation model of vehicle (Huang et al. 2016)



finite element sampling points and the uncertainty propagation is performed for the intrusion quantity I_L in the vehicle collision problem:

$$\begin{aligned}
 I_L = & 51.820X_1 - 9.242X_2 + 8.394X_3 - 79.998X_4 - 64.932X_5 \\
 & - 5.156X_1X_2 + 6.211X_2X_3 + 14.747X_1X_5 \\
 & - 5.878X_2X_4 - 9.894X_2X_5 - 8.811X_3X_4 \\
 & - 2.477X_3X_5 + 7.152X_4X_5 - 15.196X_1^2 \\
 & + 6.761X_2^2 + 20.438X_4^2 + 7.471X_5^2 + 275.327
 \end{aligned}
 \tag{34}$$

Table 5 Distribution parameters of random variables

Random variables	Weight	Mean value	Standard deviation
X_1	(0.5, 0.5)	(2.31, 2.71)	(0.09, 0.09)
X_2	(0.6, 0.4)	(2.03, 2.55)	(0.12, 0.13)
X_3	(0.4, 0.6)	(1.73, 2.13)	(0.1, 0.1)
X_4	(0.3, 0.7)	(2.22, 2.72)	(0.11, 0.1)
X_5	(0.6, 0.4)	(2.12, 2.52)	(0.11, 0.1)

Random variables are multimodal distributions based on observed data, and GMM is used to determine the probability density function of multimodal random variables. The distribution parameters of X_1, X_2, X_3, X_4 , and X_5 are listed in Table 5

Each multimodal random variable is decomposed into two random variables and five sets of random variables are constructed. Thus, a total of 32 elements are obtained in

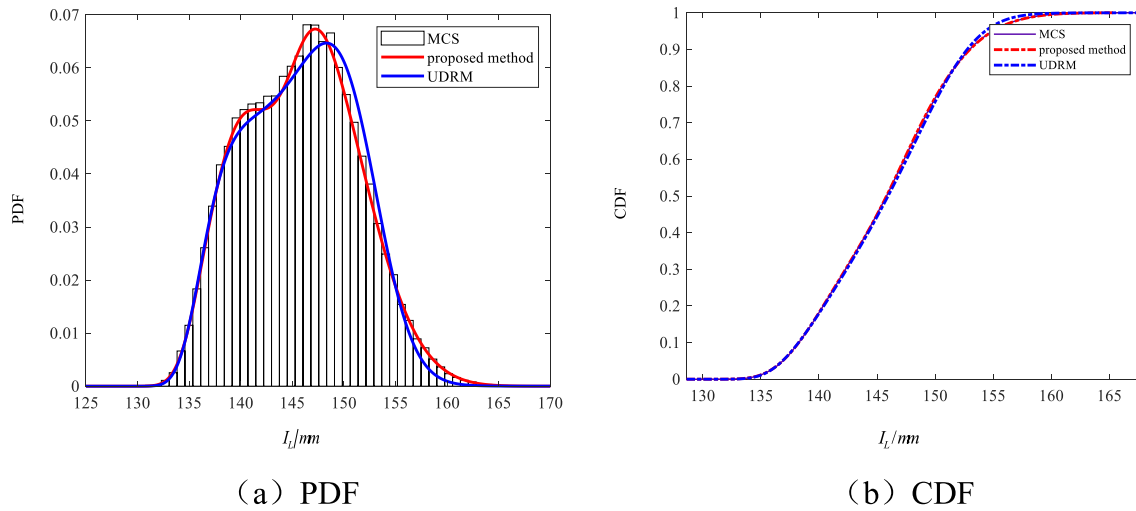


Fig. 17 The uncertainty propagation results of the proposed method, UDRM, and MCS

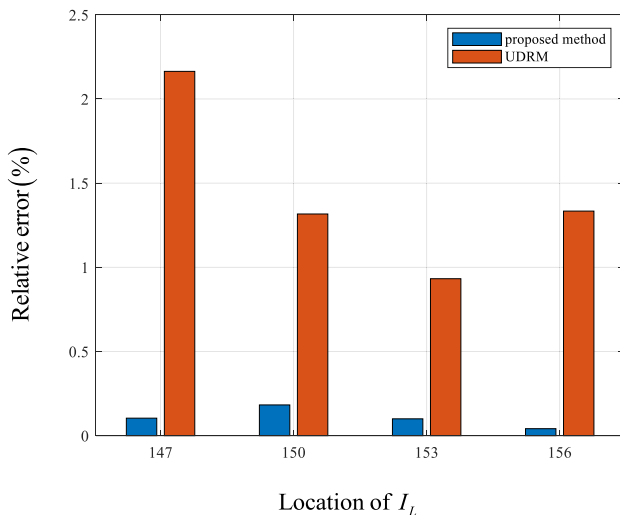


Fig. 18 Relative errors of CDF of the proposed method and UDRM

this example. The uncertainty propagation results of the proposed method are illustrated in Fig. 17.

As shown in Fig. 17, the PDF and CDF of the response function obtained by the proposed method are very close to MCS, but the results obtained by UDRM are different from MCS. In addition, the proposed method requires the first 4th-order statistical moments and UDRM requires the first 8th-order statistical moments to construct the PDF of the response function. To illustrate the computational accuracy of the proposed method, the relative errors of CDF for the proposed method and UDRM are listed in Fig. 18. Four locations ($I_L=147, 150, 153, 156$) are used to represent the computational accuracy.

The relative errors of the proposed method are smaller than that of UDRM in these locations, and their relative

errors are less than 0.5% in these locations. The highest relative error of the proposed method is located at $I_L=150$, and the highest relative error of the UDRM is located at $I_L=147$. The KLD of MCS and UDRM is 0.0085. The KLD of MCS and the proposed method is smaller, with a value of 0.0004. Hence, the proposed method has the best computational accuracy among them. The proposed method and UDRM are computationally efficient compared to MCS and they compute the response functions for 2112, 51, and 1×10^6 times, respectively. UDRM is the most computationally efficient, followed by the proposed method and MCS is the least efficient. Therefore, the proposed method has the best performance among them, considering both computational accuracy and efficiency.

6 Conclusion

This study proposes an uncertainty propagation method for multimodal distributions through unimodal decomposition strategy. First, the GMM is used to establish the probability density functions of the multimodal random variables. Second, a unimodal decomposition strategy is proposed for uncertainty propagation for multimodal distributions. A set of unimodal elements is constructed and the PDF of the response function in the elements is estimated using an arbitrary polynomial chaos expansion and the maximum entropy method. Third, the PDF of the response function in the complete probability space is obtained based on the elements. The analytical results of the three examples demonstrate that the proposed method can accurately and efficiently obtain the PDF of the response function for the

uncertainty propagation of the multimodal distribution. The proposed method avoids computing higher-order statistical moments and the first 4th-order statistical moments can meet the engineering requirements. As a result, errors in the calculation of higher-order statistical moments can be avoided. However, the limitation of this method is that more multimodal random variables or modes need to construct more elements. In this way, they lead to a decrease in computational efficiency. Further research should be done to apply the sensitivity analysis to reduce the number of input random variables and improve the computational efficiency.

Acknowledgements The research presented in this paper was conducted with the support of The National Natural Science Foundation of China (Grant No. 52235005), Fundamental Research Program of China (JCKY2020110C105), The National Science Fund for Distinguished Young Scholars (Grant No. 51725502), and The National Natural Science Foundation of China (Grant No. 52105253).

Declarations

Conflict of interest The authors declare that they have no conflict of interest.

Replication of Results The results reported in this research were performed in MATLAB. The authors will help interested researchers reproduce the results given in the article. Interested readers can contact the corresponding author for basic codes of this research with reasonable requests.

References

- Ahlfeld R, Belkouchi B, Montomoli F (2016) SAMBA: sparse approximation of moment-based arbitrary polynomial chaos. *J Comput Phys* 320:1–16
- Asquith WH (2007) L-moments and TL-moments of the generalized lambda distribution. *Comput Stat Data Anal* 51(9):4484–4496
- Au S-K, Beck JL (2001) Estimation of small failure probabilities in high dimensions by subset simulation. *Probab Eng Mech* 16(4):263–277
- Bai S, Kang Z (2021) Robust topology optimization for structures under bounded random loads and material uncertainties. *Comput Struct* 252:106569
- Bhattacharyya B (2020) Global sensitivity analysis: a Bayesian learning based polynomial chaos approach. *J Comput Phys* 415:109539
- Bhattacharyya B (2022) Uncertainty quantification and reliability analysis by an adaptive sparse Bayesian inference based PCE model. *Eng Comput* 38(2):1437–1458
- Bhattacharyya B (2023) On the use of sparse Bayesian learning-based polynomial chaos expansion for global reliability sensitivity analysis. *J Comput Appl Math* 420:114819
- Bourinet JM, Deheeger F, Lemaire M (2011) Assessing small failure probabilities by combined subset simulation and support vector machines. *Struct Saf* 33(6):343–353
- Breitung K (1984) Asymptotic approximations for multinormal integrals. *J Eng Mech* 110(3):357–366
- Castillo-Barnes D, Martínez-Murcia FJ, Ramírez J (2020) Expectation-maximization algorithm for finite mixture of α -stable distributions. *Neurocomputing* 413:210–216
- Du X (2007) Saddlepoint approximation for sequential optimization and reliability analysis. *J Mechan Design*. <https://doi.org/10.1115/1.2717225>
- Fan W, Wei J, Ang AHS (2016) Adaptive estimation of statistical moments of the responses of random systems. *Probab Eng Mech* 43:50–67
- Figueiredo MAT, Jain AK (2002) Unsupervised learning of finite mixture models. *IEEE Trans Pattern Anal Mach Intell* 24(3):381–396
- Grigoriu M, Probabilistic methods in structural engineering. In: G Augusti, A Baratta and F Casciati, Chapman and Hall - Methuen Inc., New York, 1984, pp. 556. *Structural Safety*. 4(3) (1987) 251–252.
- Guo L, Liu Y, Zhou T (2019) Data-driven polynomial chaos expansions: a weighted least-square approximation. *J Comput Phys* 381:129–145
- Hu Z, Du X (2018) Reliability Methods for Bimodal Distribution With First-Order Approximation1. *ASCE-ASME J Risk and Uncert in Engrg Sys Part B Mech Engrg*. <https://doi.org/10.1115/1.4040000>
- Hu ZL, Mansour R, Olsson M (2021) Second-order reliability methods: a review and comparative study. *Struct Multidisc Optim* 64(6):3233–3263
- Huang ZL, Jiang C, Zhou YS (2016) An incremental shifting vector approach for reliability-based design optimization. *Struct Multidisc Optim* 53(3):523–543
- Jacquelin E, Baldanzini N, Bhattacharyya B (2019) Random dynamical system in time domain: a POD-PC model. *Mech Syst Signal Process* 133:106251
- Li L, Chen G, Fang M (2021) Reliability analysis of structures with multimodal distributions based on direct probability integral method. *Reliab Eng Syst Saf* 215:107885
- Liu Y, Zhao J, Qu Z (2021a) Structural reliability assessment based on subjective uncertainty. *Int J Comput Methods* 18(10):2150046
- Liu Z, Yang M, Cheng J (2021b) A new stochastic isogeometric analysis method based on reduced basis vectors for engineering structures with random field uncertainties. *Appl Math Model* 89:966–990
- Livesey AK, Brochon JC (1987) Analyzing the distribution of decay constants in pulse-fluorimetry using the maximum entropy method. *Biophys J* 52(5):693–706
- Marseguerra M, Zio E, Devooight J (1998) A concept paper on dynamic reliability via Monte Carlo simulation. *Math Comput Simul* 47(2):371–382
- Mori Y, Kato T (2003) Multinormal integrals by importance sampling for series system reliability. *Struct Saf* 25(4):363–378
- Ni YQ, Ye XW, Ko JM (2010) Monitoring-based fatigue reliability assessment of steel bridges: analytical model and application. *J Struct Eng* 136(12):1563–1573
- Nobile F, Tempone R, Webster CG (2008) A sparse grid stochastic collocation method for partial differential equations with random input data. *SIAM J Numer Anal* 46(5):2309–2345
- Nouy A (2010) Identification of multi-modal random variables through mixtures of polynomial chaos expansions. *CR Mec* 338(12):698–703
- Oladyshkin S, Nowak W (2012) Data-driven uncertainty quantification using the arbitrary polynomial chaos expansion. *Reliab Eng Syst Saf* 106:179–190
- Pearson K, IX. Mathematical contributions to the theory of evolution.—XIX. Second supplement to a memoir on skew variation. *Philosophical Transactions of the Royal Society of London. Series A, Containing Papers of a Mathematical or Physical Character*. 216(538–548) (1916) 429–457.
- Qiao X, Wang B, Fang X (2021) Non-probabilistic reliability bounds for series structural systems. *Int J Comput Methods* 18(09):2150038

- Rahman S, Xu H (2004) A univariate dimension-reduction method for multi-dimensional integration in stochastic mechanics. *Probab Eng Mech* 19(4):393–408
- Sachdeva SK, Nair PB, Keane AJ (2006) Hybridization of stochastic reduced basis methods with polynomial chaos expansions. *Probab Eng Mech* 21(2):182–192
- Shao Q, Younes A, Fahs M (2017) Bayesian sparse polynomial chaos expansion for global sensitivity analysis. *Comput Methods Appl Mech Eng* 318:474–496
- Smolyak SA (1963) Quadrature and interpolation formulas for tensor products of certain classes of functions. *Soviet Math Dokl* 4:240–243
- Sobczyk K, Trzebicki J (1999) Approximate probability distributions for stochastic systems: maximum entropy method. *Comput Methods Appl Mech Eng* 168(1):91–111
- Tang JC, Fu CM, Mi CJ (2022) An interval sequential linear programming for nonlinear robust optimization problems. *Appl Math Model* 107:256–274
- Tian WY, Chen WW, Wang ZH (2022) An extended SORA method for hybrid reliability-based design optimization. *Int J Comput Methods*. <https://doi.org/10.1142/S0219876221500742>
- Trenkler G (1994) Continuous univariate distributions: N.L. Johnson, S. Kotz and N. Balakrishnan (2nd ed., Vol. 1). New York: John Wiley. *Computational statistics & data analysis*. 21(1) (1996) 119
- Valverde G, Saric AT, Terzija V (2012) Probabilistic load flow with non-Gaussian correlated random variables using Gaussian mixture models. *IET Gener Transm Distrib* 6(7):701–709
- Wang R, Luo Y (2019) Efficient strategy for reliability-based optimization design of multidisciplinary coupled system with interval parameters. *Appl Math Model* 75:349–370
- Wu SQ, Law SS (2012) Statistical moving load identification including uncertainty. *Probab Eng Mech* 29:70–78
- Wu J, Zhang D, Jiang C (2021) On reliability analysis method through rotational sparse grid nodes. *Mech Syst Signal Process* 147:107106
- Xu H, Rahman S (2004) A generalized dimension-reduction method for multidimensional integration in stochastic mechanics. *Int J Numer Meth Eng* 61(12):1992–2019
- Yang M, Zhang D, Cheng C (2021) Reliability-based design optimization for RV reducer with experimental constraint. *Struct Multidisc Optim* 63(4):2047–2064
- Zeng YC, Song DL, Zhang WH (2020) Stochastic failure process of railway vehicle dampers and the effects on suspension and vehicle dynamics. *Vehicle Syst Dyn*. <https://doi.org/10.1080/00423114.2019.1711136>
- Zhang Z, Jiang C, Han X (2019) A high-precision probabilistic uncertainty propagation method for problems involving multimodal distributions. *Mech Syst Signal Process* 126:21–41
- Zhao Q, Guo J, Hong J (2019) Closed-form error space calculation for parallel/hybrid manipulators considering joint clearance, input uncertainty, and manufacturing imperfection. *Mech Mach Theory* 142:103608

Publisher's Note Springer Nature remains neutral with regard to jurisdictional claims in published maps and institutional affiliations.

Springer Nature or its licensor (e.g. a society or other partner) holds exclusive rights to this article under a publishing agreement with the author(s) or other rightsholder(s); author self-archiving of the accepted manuscript version of this article is solely governed by the terms of such publishing agreement and applicable law.

Authors and Affiliations

Boqun Xie¹ · Chao Jiang¹  · Zhe Zhang¹ · Jing Zheng¹ · Jinwu Li¹

✉ Chao Jiang
jiangc@hnu.edu.cn

and Vehicle Engineering, Hunan University, Changsha, China

¹ State Key Laboratory of Advanced Design and Manufacturing for Vehicle Body, College of Mechanical